# Supporting Information

## Pt−Co Truncated Octahedral Nanocrystals: A Class of Highly Active and Durable Catalysts toward Oxygen Reduction

*Min Shen,[a,b+] Minghao Xie,[c+] John Slack,[d] Krysta Waldrop,[d] Zitao Chen,[a] Zhiheng Lyu,[c] Shaohong Cao,[e] Ming Zhao,[c] Miaofang Chi,[e] Peter N. Pintauro,[d] Rong Cao,[b] and Younan Xia[a,c*]*

[a]The Wallace H. Coulter Department of Biomedical Engineering, Georgia Institute of Technology and Emory University, Atlanta, Georgia 30332, United States

[b]State Key Laboratory of Structural Chemistry, Fujian Institute of Research on the Structure of Matter, Chinese Academy of Sciences, Fuzhou 350002, China

[c]School of Chemistry and Biochemistry, Georgia Institute of Technology, Atlanta, Georgia 30332, United States

[d]Department of Chemical and Biomolecular Engineering, Vanderbilt University, Nashville, Tennessee 37235, United States

[e]Center for Nanophase Materials Sciences, Oak Ridge National Laboratory, Oak Ridge, Tennessee 37831, United States

[+] These authors contributed equally to this work.

[*]Corresponding author. E-mail: younan.xia@bme.gatech.edu

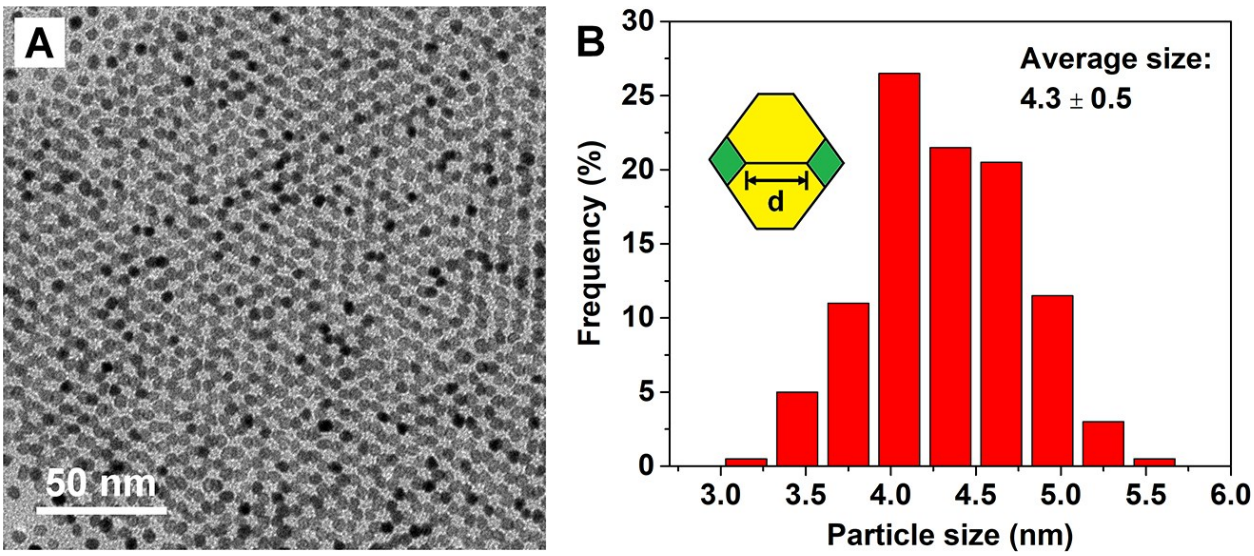


**Fig. S1.** (A) TEM image and (B) size distribution of the as-synthesized Pt−Co TONs with an average size of 4.3 ± 0.5 nm. The inset in (B) shows a schematic of the Pt−Co TON, together with the definition of size.

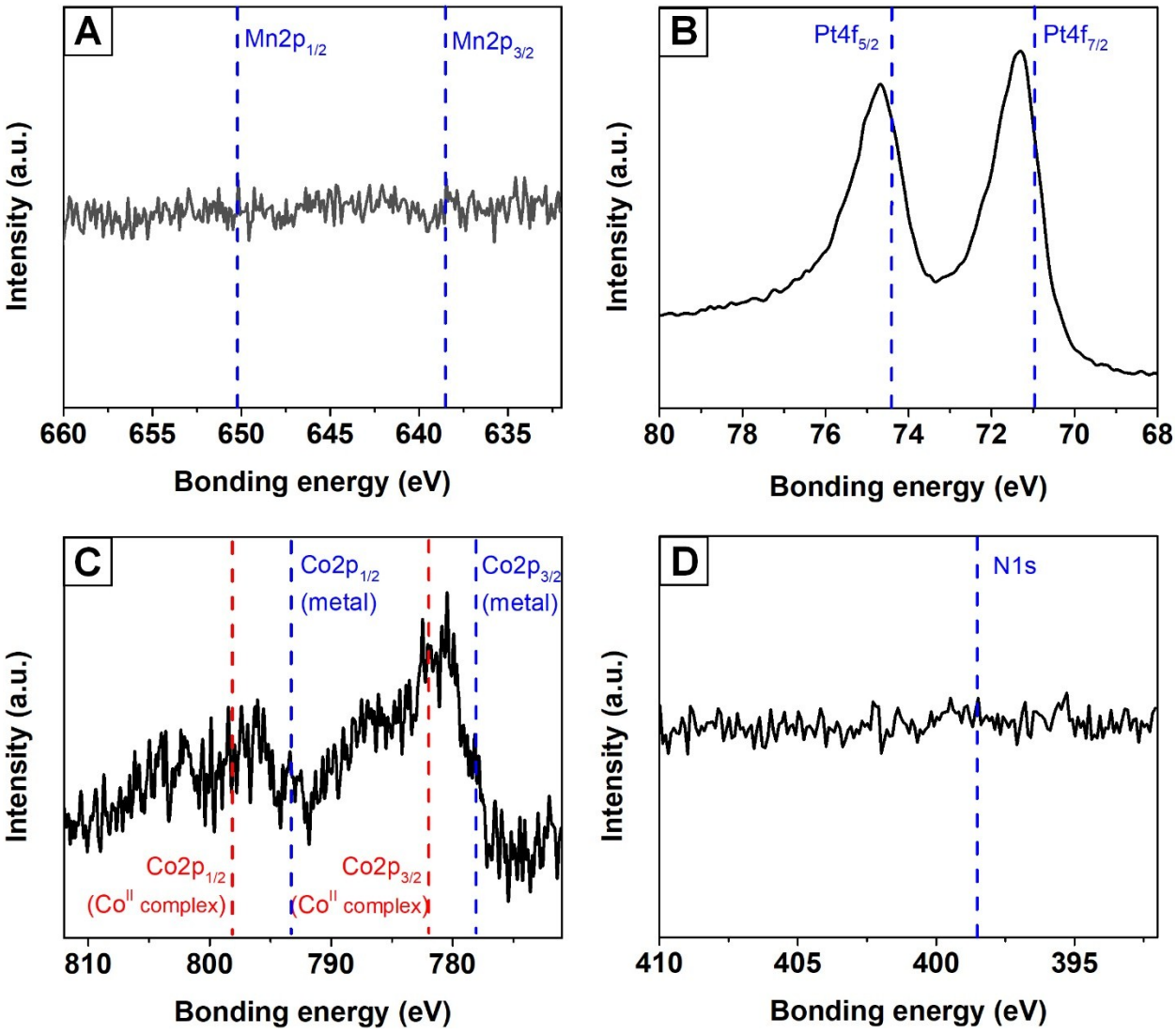


**Fig. S2.** XPS spectra of the Pt−Co TONs: (A) Mn 2p, (B) Pt 4f, (C) Co 2p, and (D) N 1s.

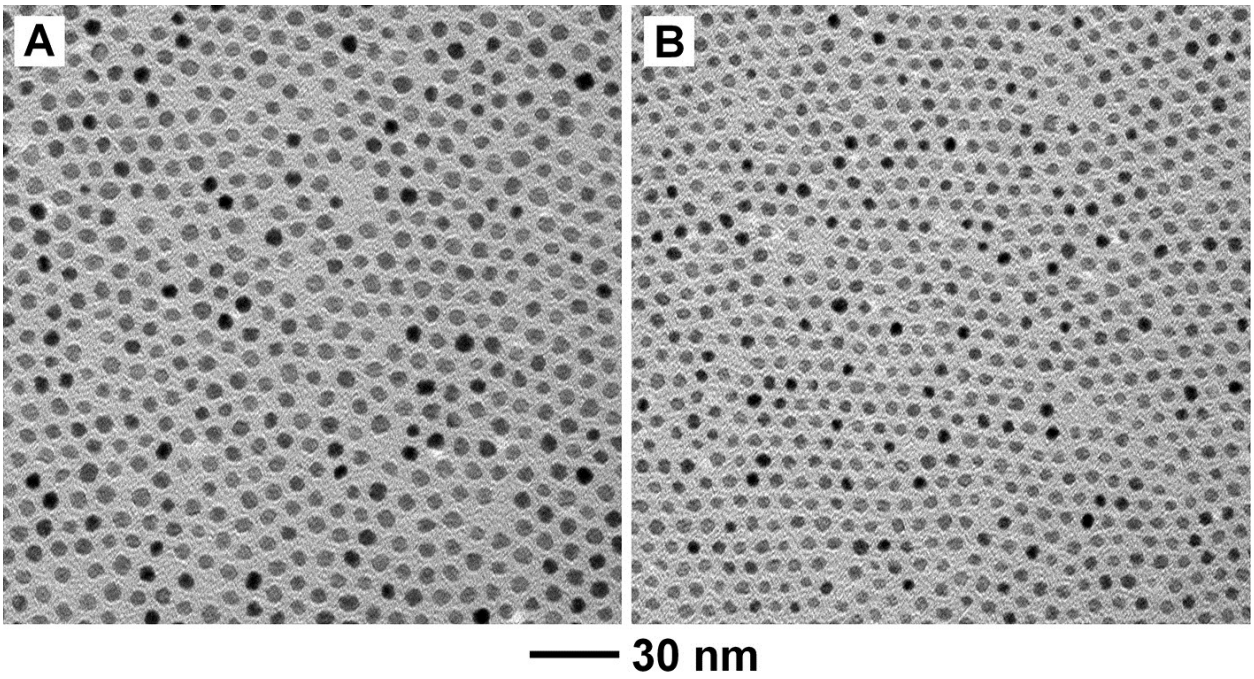


**Fig. S3.** TEM images of the Pt−Co nanocrystals prepared using the standard protocol except for the variation in reaction temperature: (A) 180 and (B) 210 $^{o}$C, respectively.

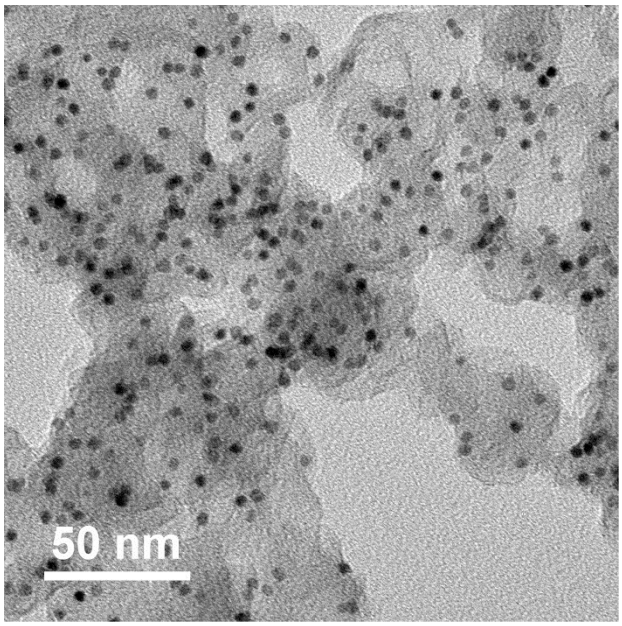


**Fig. S4.** TEM image of the pristine Pt−Co TONs/C with a Pt mass loading of *ca.* 17.6%.

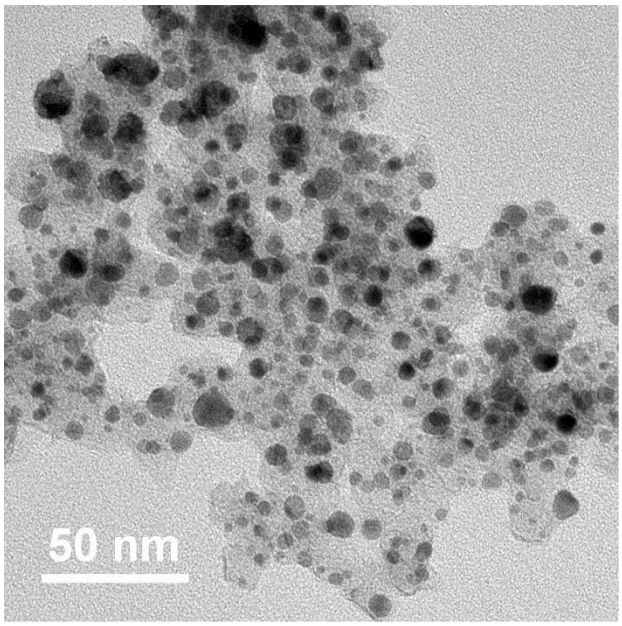


**Fig. S5.** TEM image of the pristine TKK $Pt_3Co/C$ with a Pt mass loading of 48.6%.

**Table S1.** Variation of the elemental compositions of the Pt−Co nanocrystals when adjusting the amount of $CHCl_3$ at different feeding ratios for the precursors. The elemental compositions were determined using ICP-MS.

| experimental conditions | | | | | | | Pt/Co atomic ratio |
|---|---|---|---|---|---|---|---|
| **$Pt(acac)_2$ /mmol** | **$Co(acac)_2$ /mmol** | **$Mn_2(CO)_{10}$ /mmol** | **OAm /mL** | **OAc /mL** | **BE /mL** | **$CHCl_3$ /mL** | |
| 0.31 | 3.1 | 0.62 | 12 | 6.0 | 42 | 6.0 | 6.4 |
| 0.31 | 3.1 | 0.62 | 12 | 6.0 | 42 | 5.0 | 4.4 |
| 0.31 | 3.1 | 0.62 | 12 | 6.0 | 42 | 4.0 | 2.6 |
| 0.31 | 3.1 | 0.62 | 12 | 6.0 | 42 | 3.0 | 1.7 |
| 0.31 | 4.6 | 0.62 | 12 | 6.0 | 42 | 6.0 | 2.2 |
| 0.31 | 4.6 | 0.62 | 12 | 6.0 | 42 | 5.0 | 1.7 |
| 0.31 | 4.6 | 0.62 | 12 | 6.0 | 42 | 4.0 | 1.6 |
| 0.31 | 4.6 | 0.62 | 12 | 6.0 | 42 | 3.0 | 0.8 |

**Table S2.** Comparison of the ECSAs, SAs, and MAs toward ORR for the $Pt_{2.6}Co$ TONs/C, Premetek Pt/C, and TKK $Pt_3Co$/C catalysts in the liquid half-cell test.

| | **specific $ECSA_H$ ($m^2\ g_{Pt}^{-1}$)** | **$SA_H$ at 0.85 V ($mA\ cm^{-2}$)** | **$MA_{Pt}$ at 0.85 V ($A\ g_{Pt}^{-1}$)** |
|---|---|---|---|
| **Premetek Pt/C** | 25.1 | 0.84 | 210 |
| **TKK $Pt_3Co$/C** | 20.1 | 1.34 | 270 |
| **$Pt_{2.6}Co$ TONs/C** | 23.8 | 1.30 | 310 |

**Table S3.** MEA performance of the $Pt_{2.6}Co$ TONs/C catalyst during the AST.

| | **$MA_{Pt}$ at 0.9 V ($A\ g_{Pt}^{-1}$)** | **specific $ECSA_H$ ($m^2\ g_{Pt}^{-1}$)** | **max power density ($mW\ cm^{-2}$)** | **power density at 0.65 V ($mW\ cm^{-2}$)** |
|---|---|---|---|---|
| **initial** | 372 | 83.2 | 704 | 628 |
| **after 1,000 cycles** | 340 | 80.7 | 716 | 651 |
| **after 5,000 cycles** | 302 | 77.9 | 731 | 653 |
| **after 10,000 cycles** | 288 | 72.2 | 714 | 620 |
| **after 30,000 cycles** | 224 | 68.7 | 678 | 612 |

**Table S4.** Comparison of $Pt_{2.6}Co$ TONs/C and TKK $Pt_3Co$/C catalysts before and after the AST.

| | **$MA_{Pt}$ at 0.9 V (A $g_{Pt}^{-1}$)** | | **max power density (mW $cm^{-2}$)** | |
|---|---|---|---|---|
| | **$Pt_{2.6}Co$ TONs/C** | **TKK $Pt_3Co$/C** | **$Pt_{2.6}Co$ TONs/C** | **TKK $Pt_3Co$/C** |
| **BOL** | 294 | 230 | 707 | 593 |
| **BOL + recovery** | 384 (R4)[a] | | 704 | |
| **EOL** | 224 | 138 | 678 | 247 |
| **EOL + recovery** | 335 (R2)[a] | | 692 (R2)[a] | |

[a]The highest value over the recovery cycles (R4: the 4th cycle of recovery, R2: the 2nd cycle of recovery).